CALCULATION OF A TWISTED GASEOUS SCREEN IN A CYLINDRICAL CHANNEL

É. P. Volchkov, N. A. Dvornikov, and
V. I. Terekhov

UDC 532.526.4:536.24

The effectiveness of a twisted gaseous screen in a cylindrical channel and heat and mass transfer under such conditions were studied experimentally in [1-3], where a number of characteristic features, as compared with the nontwisted screen, determined by the rotation of the peripheral part of the flow were established. In particular, it is shown in [1] that increasing the injection parameter of the inert gas $m = \rho_s w_s/\rho_0 w_0$ in the presence of twisting, unlike the nontwisted screen, intensifies the mass transfer processes. At the same time, flows with partial peripheral twisting differ from completely twisted flows. The main difference consists of the fact that in the presence of peripheral twisting of the flow a typical jet circulation profile with two characteristic zones – the zone near the wall and an exterior zone – develops. In the part of the circulation profile near the wall ($y < \delta_m$, Fig. 1), like in completely twisted flows owing to the interaction with the wall, the circulation deceases ($d\Gamma/dr < 0$), which in its turn intensifies heat and mass transfer processes. In the jet part of the boundary layer ($\delta_m < y < \delta$) the circulation increases in the radial direction ($d\Gamma/dr > 0$) and the turbulent transport by centrifugal forces is suppressed, which can reduce heat flows from the core of the flow to the wall [1]. This phenomenon is widely employed for thermal shielding of walls and stabilization of arcs in plasma reactors [5]. So, the magnitude of the heat flux in channels with peripheral twisting is determined primarily by two factors – intensification of heat transfer in the part of the boundary layer near the wall and suppression of the external part in it. Correspondingly, depending on the specific conditions, the rotation of the peripheral flow can both increase and decrease the coefficients of turbulent heat and mass transfer on the surface of the channel.

In this paper the dynamics and heat and mass transfer are analyzed for a flow with a twisted screen near the wall with $m < 1$. Taking into account all of the above-indicated factors substantially increases the complexity of the calculation of the parameters of the twisted screen. Therefore, in order to obtain the final analytic expressions, a number of simplifying assumptions are adopted in the solution; the main factors, determining the process of development of a rotating jet in a cylindrical channel, are, however, taken into account here.

1. Integral Energy and Momentum Relations for a Twisted Screen. Consider a twisted jet, developing in a cylindrical channel in the presence of a comoving untwisted flow at its center, near the wall. A diagram of the flow is shown in Fig. 1. The jet is injected through a gap of height s and has an initial twist angle of φ_s. For small injection parameters ($m < 1$), owing to the interaction of the jet with the main flow, the twist angle of the flow at the wall will decrease quite rapidly along the channel.

The basic parameters of the problem under study to be determined are the distribution of the temperature of the adiabatic surface (effectiveness of the screen), and also the heat and mass fluxes in the presence of heat and mass transfer at the wall. For a rotating jet near the wall the unknown quantity is the change in the twist angle of the flow at the wall along the channel. For this reason, in the case under study, the integral equations for the momentum, the angular momentum, and the energy must be solved simultaneously.

It is easy to show that the integral relation for the energy for a twisted gaseous screen on an adiabatic surface ($q_w = 0$) is identical to the analogous dependence for a screen with no twisting [6]

$$d(\theta\delta_T^{**})/dz = 0. \tag{1.1}$$

Novosibirsk. Translated from Zhurnal Prikladnoi Mekhaniki i Tekhnicheskoi Fiziki, No. 4, pp. 59-68, 1986. Original article submitted June 3, 1985.

 0021-8944/86/2704-0530$12.50

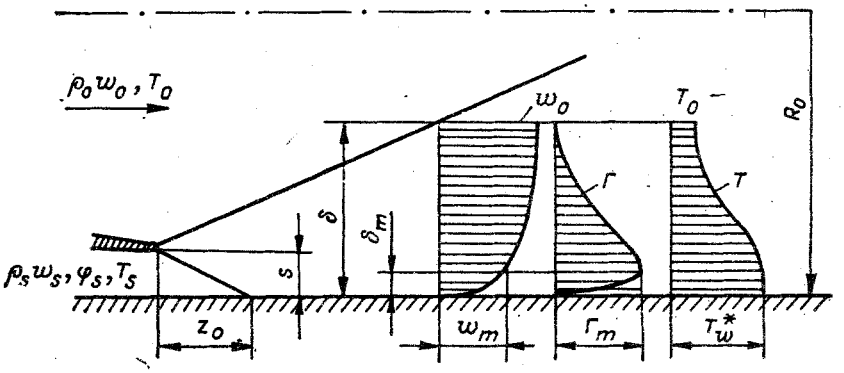

Fig. 1

Equation (1.1) was obtained under the condition that the longitudinal velocity in the core of the flow w_0 is constant. Here $\theta = (T_0 - T_w^*)/(T_0 - T_s)$ is the effectiveness of the gas screen, while T_s, T_0 and T_w^* are the temperature of the gas in the gap, in the core of the flow, and on the adiabatic surface. The thickness of the energy loss layer is determined by

$$\delta_T^{**} = \int_0^{\delta_T} \frac{\rho w}{\rho_0 w_0}(1-\eta)\left(1-\frac{y}{R_0}\right)dy. \tag{1.2}$$

where $\eta = (T - T_w^*)/(T_0 - T_w^*)$ is the dimensionless temperature in the boundary layer.

An integral equation for the conversion of angular momentum can be obtained in a similar manner from the differential equation of motion in a circular direction, taking into account the boundary conditions in the core of the flow $r = R_0 - \delta$, $w = w_0$, $\Gamma = vr = 0$, $u = 0$, $\tau_\phi = 0$ and at the wall of the channel $r = R_0$, $w = 0$, $u = 0$, $v = 0$, $\phi_\tau = \tau_{\phi w}$:

$$\frac{d}{dz}\int_0^{\delta} \rho w \Gamma\left(1-\frac{y}{R_0}\right)dy = \tau_{\varphi w} R_0. \tag{1.3}$$

From here, neglecting the losses owing to friction against the surface of the channel in the circulation direction $\tau_{\phi w} = 0$, for a zero gradient flow ($dw_0/dz = 0$) from (1.3) we obtain

$$d\left(\bar{\Gamma}_m \delta_\varphi^{**}\right)/dz = 0. \tag{1.4}$$

Here $\bar{\Gamma}_m = \Gamma_m/\Gamma_s$; $\Gamma_s = v_s R_0$ is the circulation of the flow in the gap for $s \ll R_0$; and w, v, and u are the longitudinal, azimuthal, and radial components of the velocity.

The thickness of the angular-momentum loss layer is determined by the expression

$$\delta_\varphi^{**} = \int_0^{\delta_\varphi} \frac{\rho w}{\rho_0 w_0}\frac{\Gamma}{\Gamma_m}\left(1-\frac{y}{R_0}\right)dy. \tag{1.5}$$

Comparison of the experimental distributions of the temperatures and circulations in the jet part of the boundary layer of the twisted gaseous screen showed [3] that these profiles are similar to one another and can be described by jet dependences, in particular, by Schlichting's formula

$$\Gamma/\Gamma_m = 1 - \eta = (T - T_0)/(T_w^* - T_0) = (1 - \xi^{1,5})^2$$
$$(\xi = (R_0 - r)/\delta = y/\delta).$$

Comparison of (1.2) and (1.5) shows that when the thicknesses of the thermal and dynamic boundary layers are the same ($\delta_T = \delta_\phi = \delta$), the integral scales also are the same ($\delta_T^{**} = \delta_\phi^{**}$). Taking this fact into account, after integrating (1.1) and (1.4) we obtain

$$\Gamma_m/\Gamma_s \equiv \theta_\varphi = \theta = \delta_{Ts}^{**}/\delta_T^{**} = \delta_{\varphi s}^{**}/\delta_\varphi^{**}. \tag{1.6}$$

where $\theta_\phi = \Gamma_m/\Gamma_s$ is the change in the maximum circulation along the channel; $\delta^{**}_{Ts} = \delta^{**}_{\phi s} = ms(1 - s/2\,R_0) \approx ms$ are the integral parameters on the cutoff of the gap.

The relations (1.6) imply the important result that the maximum value of the circulation in the boundary layer of the twisted screen Γ_m/Γ_s decreases along the channel just like the dimensionless temperature of the adiabatic wall, if the frictional losses of twisting of the flow are neglected, i.e., in this case the change in the circulation Γ_m along the channel owing only to the mixing or the twisted peripheral flow with the untwisted main flow is taken into account. Then it is sufficient to find the change in the angle of twist of the flow at the wall, whose value also determines the intensity of the transport processes in the boundary layer. Assuming that the circulation profile in the part near the wall ($y < \delta_m$), like the profile of the longitudinal component of the velocity, is described by the same power-law dependence (this is equivalent to a constant angle of twist along the thickness of the given zone), from (1.6) we obtain

$$\operatorname{tg}\varphi_m/\operatorname{tg}\varphi_s = \frac{\Gamma_m}{\Gamma_s}\frac{w_s/w_0}{(\delta_m/\delta)^n} = \theta_\varphi\,(\delta/\delta_m)^n\,(w_s/w_0)_*. \tag{1.7}$$

where ϕ_m and ϕ_s are the angle of twist at the wall in the section under study and at the cutoff of the slit, and n is the exponent in the power law for the distribution of the velocity $w/w_0 = (y/\delta)^n$. When the screen is twisted, the quantity n differs from the value for the standard boundary layer $n_0 = 1/7$, and depends on the magnitude of the effect of the mass forces on the turbulent transport.

We shall determine the change in the effectiveness of the gaseous screen and of the maximum circulation along the channel by the method developed in [6] for gaseous screens on a plate, and we shall employ this method in the analysis of the twisted screen. Since the equation of conservation of momentum in the longitudinal direction for a twisted flow has the same form as the integral equation for the momentum when there is no twisting [7], we shall write the expression for the effectiveness of the screen in a manner analogous to the expression for the flow on the plate [6]

$$\theta = \left[1 + 0{,}25\,(\beta/\beta_0)^{1{,}25}\,\mathrm{Re}_s^{-0{,}25}\frac{1}{ms}\int_{z_0}^{z}\Psi_\varphi\Psi_c\Psi_T\,(\mu_w/\mu_0)^{0{,}25}\,dz\right]^{-0{,}8}. \tag{1.8}$$

Here z_0 is the length of the initial section, where $\theta = 1$; $\mathrm{Re}_s = \rho_s w_s s/\mu_s$.

Taking into account the similarity of the circulations and temperatures in the twisted screen, the expression for the angle of twist along the channel has the same form as (1.8):

$$\operatorname{tg}\varphi_m = \operatorname{tg}\varphi_s\left[1 + 0{,}25(\beta/\beta_0)^{1{,}25}\frac{1}{ms}\left(\frac{w_0}{w_s}\right)^{1{,}25}\left(\frac{\delta_m}{\delta}\right)^{1{,}25n}\mathrm{Re}_s^{-0{,}25} \times\int_{z_0}^{z}\Psi_T\Psi_c\Psi_\varphi\left(\frac{\mu_w}{\mu_0}\right)^{0{,}25}dz\right]^{-0{,}8}. \tag{1.9}$$

The effect of the rotation of the peripheral part of the flow on the effectiveness of the screen and the damping of the twisting in (1.8) and (1.9) is manifested through the ratio of the coefficients β/β_0 and the relative friction functions, determined by the increase in the velocity vector owing to the twisting (Ψ_ϕ), and also through the effect of mass forces on the turbulent transport. According to [7], the latter quantities are determined by the relations

$$\Psi_\varphi = 1/\cos\varphi_m^{0{,}75}; \tag{1.10}$$

$$\Psi_c = \left\{1 + 1{,}8\cdot10^3\frac{\delta^{**}}{R_0}\sin^2\varphi_m\frac{\delta_m}{\delta}\left[1 + \frac{\psi - 1}{2\,(\psi n + 1)}\right]\right\}^{0{,}162}. \tag{1.11}$$

The expression (1.11) is valid for a boundary layer on a convex surface in the presence of a twisted screen. The function of nonisothermality is written in (1.8) and (1.9) in the standard fashion [6]: $\Psi_T = [2/(\sqrt{\psi} + 1)]^2$, where $\psi = T^*_w/T_0$ is the temperature factor.

In the relations (1.8) and (1.9) $\beta = \delta_T^{**}/\delta^{**}$ (δ^{**} is the thickness of the momentum loss in the longitudinal direction). In the limit $Re \to \infty$ the expression for β, for a sufficiently thin boundary layer $\delta/R_0 \ll 1$, has the same form as for a nontwisted screen [6]

$$\beta = \int_0^1 \bar{\rho}\omega d\xi \Big/ \int_0^1 \bar{\rho}\omega(1-\omega)d\xi. \tag{1.12}$$

For a nontwisted screen under isothermal conditions $\bar{\rho} = \rho/\rho_0 \approx 1$ and $\omega_0 = \xi^{1/7}$ from (1.12) $\beta_0 = 9$. In the general case the rotation of the screen will be manifested in β through the profile of the longitudinal velocity, whose filling depends on the magnitude of the effect of the mass forces on the turbulent transport.

2. Effect of Mass Forces on the Longitudinal Velocity Profile in the Twisted Screen. We shall determine the effect of different factors on the longitudinal velocity profile. The expression for the longitudinal component of the tangential stress in a three-dimensional boundary layer is given by

$$\tau_z = \rho l_0^2 \left(\frac{\partial w}{\partial r}\right)^2 \left[1 + \left(\frac{\frac{1}{r}\frac{\partial \Gamma}{\partial r}}{\partial w/\partial r}\right)^2\right]^{1/2} f. \tag{2.1}$$

The function f in (2.1) takes into account the effect of mass forces on turbulence in the boundary layer [8]. In the twisted gaseous screen, as indicated above, there are two characteristic zones in which the mass forces act in opposite directions. In the part near the wall ($0 < y < \delta_m$) the circulation decreases in the radial direction, which intensifies the turbulent transport, and in addition [8]

$$f = \sqrt{1 - (y/l_0)^2 \mathrm{Ri}}. \tag{2.2}$$

In the exterior region ($\delta < y < \delta_m$) $d\Gamma/dr > 0$ and turbulent transport is suppressed. The quantity f in this zone is calculated [8] as

$$f_{ext} = 1\sqrt{1 + (y/l_0)^2\,\mathrm{Ri}}. \tag{2.3}$$

Richardson's number in (2.2) and (2.3) is [8]

$$\mathrm{Ri} = \left(\frac{2\Gamma}{r^3}\frac{\partial \Gamma}{\partial r} + \frac{1}{\rho}\frac{\partial \rho}{\partial r}\frac{\Gamma^2}{r^3}\right) \Big/ \left[\left(\frac{\partial w}{\partial r}\right)^2 + \left(\frac{1}{r}\frac{\partial \Gamma}{\partial r}\right)^2\right]. \tag{2.4}$$

The calculation of the characteristics of the boundary layer from Eq. (2.1) must correspondingly be carried out for two regions: the region near the wall and the exterior region.

Because of the fact that the thickness of the zone near the wall is much smaller than the thickness of the exterior zone ($\delta_m/\delta \ll 1$) however, the effect of the near-wall zone on the exterior zone is insignificant, and the calculation of the velocity distribution over the thickness of the latter can be carried out taking into account only the suppression of the turbulent transport in the jet part of the boundary layer.

Then Eq. (2.1) can be put into the form

$$\frac{\partial \omega}{\partial \xi} = \frac{\partial \omega_0}{\partial \xi}\sqrt{\frac{\Psi_\varphi \Psi_c \Psi_T}{\bar{\rho} f_\varphi f_{ext}}}. \tag{2.5}$$

The velocity profile in the standard boundary layer is given by $\omega_0 = \xi^{1/7}$.

The function reflecting the increase in the gradient of the flow velocity in the exterior part of the screen, according to (2.1), equals

$$f_\varphi = \left[1 + \left(\frac{\frac{1}{r}\frac{d\Gamma}{dr}}{\frac{\partial w}{\partial r}}\right)^2\right]^{1/2} \approx \frac{1}{\cos \varphi_m},$$

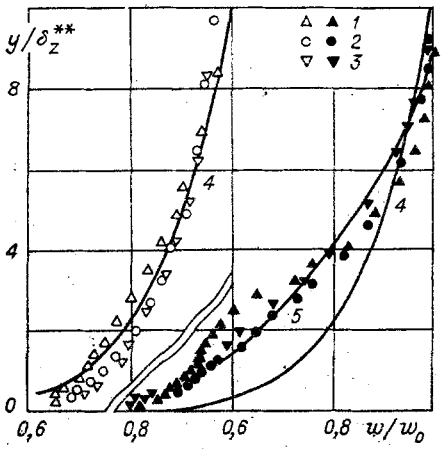

Fig. 2

while the effect of the mass forces on the suppression of the turbulent transport in this zone is described by the formula (2.3). To a first approximation it may be assumed that $f_\phi \approx \Psi_\phi$, and the possible error in using this form is insignificant here, since rapid decay of the twisting is characteristic for the screen and $\Psi_\phi \approx f_\phi \to 1$.

The expression (2.4) can be put into the form [7]

$$\mathrm{Ri} \approx \frac{\delta \sin^2 \varphi_m}{R_0}\left[1 - \frac{\psi - 1}{4(\psi n + 1)}\right]. \tag{2.6}$$

Then assuming that $(y/l_0)^2 \approx (\delta/l_0)^2 = 1/c_0^2$, the expression for the function expressing the suppression of turbulence in the exterior part of the layer (2.3), taking into account (2.6), can be written as

$$f_{\mathrm{ext}} = 1\Big/\sqrt{1 + \frac{\delta \sin^2 \varphi_m}{R_0 c_0^2}\left[1 - \frac{\psi - 1}{4(\psi n + 1)}\right]}. \tag{2.7}$$

It may be assumed [9] that in the exterior part of the boundary layer $c_0 \approx 0.09$.

We shall determine from (2.5) the exponent n in the law governing the variation of the longitudinal velocity $\omega = \xi^n$, assuming that in the exterior part of the boundary layer $\rho \cong 1$:

$$n = n_0 \xi^{n_0 - n} \sqrt{\Psi_c \Psi_T / f_{\mathrm{ext}}}. \tag{2.8}$$

Since in the exterior part of the boundary layer $\xi^{n_0 - n} \to 1$, (2.8) assumes the form

$$n = n_0 \sqrt{\Psi_c \Psi_T / f_{\mathrm{ext}}}. \tag{2.9}$$

In spite of the quite severe simplifications, the dependence (2.9) satisfactorily describes the effect of mass forces on the filling of the velocity profile in the boundary layer of the twisted gaseous screen. Figure 2 shows the experimental data [10, 11] on the distribution of the axial component of the velocity in the presence of the untwisted (light circles) and twisted $\phi_s = 74°$ (dark circles) screens. The injection parameter m = 0.5, and the distance from the cutoff of the slit is z/s = 48, 93, and 147 (points 1-3).

It is well-known [10] that in a nontwisted gaseous screen the nonuniformity of the velocity profile in the starting sections, caused by the injection, vanishes rapidly downstream and the velocity distribution assumes the form of the standard power-law profile for a turbulent boundary layer. This is also confirmed by the data in Fig. 2 (light circles), where the line 4 shows the computed dependence for the standard boundary layer $n_0 = 1/7$.

A similar picture is to be expected under conditions of twisting of the screen, especially since the effectiveness of the mixing of the jet near the wall with the main flow would appear to be higher owing to the twisting. As follows from Fig. 2, however, the suppression of turbulence in the exterior part of the boundary layer predominates in this case, and this

TABLE 1

φ_m, deg	Ψ_φ	Ψ_c	f_{ext}	n	β/β_0	$(\beta/\beta_0)^{1,25}\times$ $\times\Psi_\varphi\Psi_c$
0	1	1	1	0,142	1	1
10	1,01	1,02	0,85	0,156	0,93	0,94
20	1,05	1,06	0,64	0,184	0,83	0,87
30	1,11	1,11	0,49	0,214	0,74	0,85
45	1,29	1,18	0,37	0,25	0,66	0,91
60	1.68	1.24	0.31	0.28	0.61	1.12

reduces the filling of the longitudinal velocity profile.

According to the calculation, for a twisted screen with m = 0.5, $\phi_s = 74°$, and $z/s \approx 100$ the exponent in the power law of the velocity (2.9) $n \approx 0.26$ and remained virtually constant along the channel. The line 5 in Fig. 2 shows the computed profile for these conditions. It is evident that the computed curve falls along the experimental points, and the experimental points deviate from the curve for the standard boundary layer.

The results of the calculations based on the formulas (1.10), (1.11), (2.7), and (2.9) with $\delta/R_0 = 0.1$ are presented in Table 1, whence it follows that the twisting of the screen appreciably changes the friction, degree of suppression of the turbulent transport f_{ext}, and the coefficient β. However, the complex $(\beta/\beta_0)^{1,25}\Psi_\varphi\Psi_c\Psi_T(\mu_w/\mu_0)^{0,25}$, determining the effectiveness of the screen according to the expressions (1.8) and (1.9), changes insignificantly. A similar tendency is also observed for other ratios δ/R_0 for nonisothermal flows. This important fact enables substantial simplification of the analysis of the effectiveness and the dynamics of the twisted screen and the calculation of quantities to a first approximation neglecting deviations from isothermal conditions, twisting, mass forces, and other factors.

Then the dependences (1.8) and (1.9) will assume the form

$$\theta = \left(1 + 0{,}25\frac{z - z_0}{ms}\mathrm{Re}_s^{-0,25}\right)^{-0,8}; \tag{2.10}$$

$$\mathrm{tg}\,\varphi_m/\mathrm{tg}\,\varphi_s = \left[1 + 0{,}25\frac{z - z_0}{ms}\left(\frac{w_0}{w_s}\right)^{1,25}\left(\frac{\delta_m}{\delta}\right)^{1,25n}\mathrm{Re}_s^{-0,25}\right]^{-0,8}. \tag{2.11}$$

The weak effect of the twisting on the effectiveness of the thermal screen, calculated taking into account the length of the initial section, is shown experimentally in [2].

Figure 3 shows the generalization of the experimental data [2] on the effectiveness of the twisted screen (dark points) and the decay of circulation along the channel (light points). The experimental data in Fig. 2 correspond to the following experimental conditions: *1* — $\varphi_s = 58°$, $m = 0{,}3$; *2* — 58°, 0,5; *3* — 58°, 0,9; *4* — 74°, 0,3; *5* — 74°, 0,5; *6* — 58°, 0,3; *7* — 58°, 0,5; *8* — 58°, 0,9; *9* — 74°, 0.3; *10* — 74°, 0,5; *11* — 74°, 0.9; *12* — 0°, 0,3; *13* — 0°, 0.5. The points 12 and 13 correspond to experiments on the effectiveness for a nontwisted screen. In the experiments of [2] the angles of twist of the flow at the wall were measured, so that the experimental data on the decay of the maximum circulation were determined using the expression (1.7). In so doing it was assumed that n = 1/7 and $\delta_m/\delta = 0.21$, the latter was obtained from the solution of the integral momentum equation for the twisted screen [7]. The length of the initial section, owing to its shortness, was assumed to equal $z_0 = 0$ in the calculation. The experimental results for the twist angle and the thermal efficiency are the same, indicating the similarity of heat and angular momentum transport processes in twisted screens. The same data agree with the experimental points for the nontwisted screen and the results of the calculations based on the formula (2.10) (the line in Fig. 3), which confirms the possibility of using the simplified dependences (2.10) and (2.11) for the calculations.

3. Heat and Mass Transfer in a Boundary Layer with a Twisted Screen. The coefficient of heat and mass transfer on the surface in the presence of a twisted screen can be determined from the formula

$$\mathrm{St} = \Psi\mathrm{St}_0 = \Psi_\varphi\Psi_c\Psi_T\mathrm{St}_0. \tag{3.1}$$

Here $\mathrm{St} = q_w/\rho_0 w_0 c_p(T_w - T_w^*)$; Ψ_φ, Ψ_c, Ψ_T are the relative coefficients of heat and mass transfer, determined by the effect of the twisting of the flow, the centrifugal forces, and the

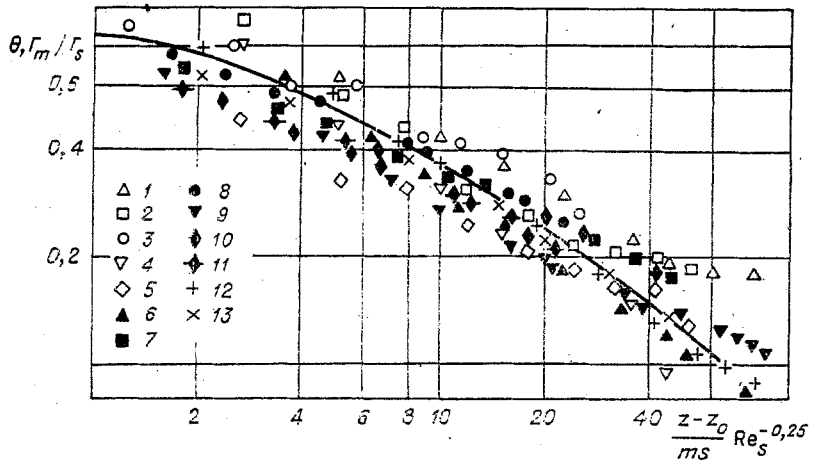

Fig. 3

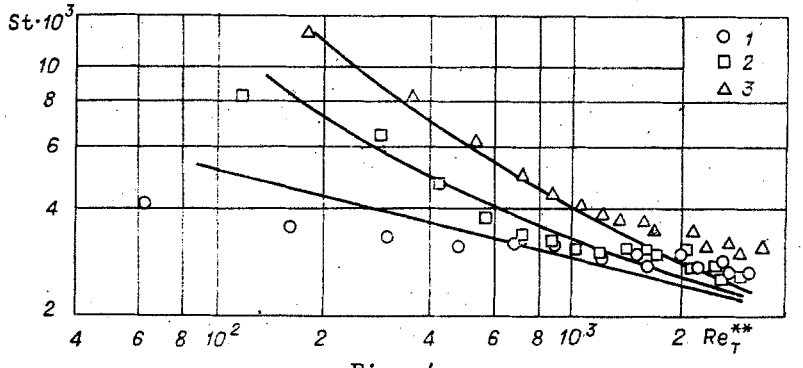

Fig. 4

nonisothermality. These quantities, by analogy with friction and heat and mass transfer in a twisted flow [7], are identical to the similar dependences for the friction (1.10) and (1.11). Stanton's number under standard conditions is calculated based on the formula

$$\mathrm{St}_0 = 0.0128\,\mathrm{Re}_T^{**-0,25}\,\mathrm{Pr}^{-0,75}\left(\frac{\mu_w}{\mu_0}\right)^{0,25}, \tag{3.2}$$

where $\mathrm{Re}_T^{**} = \rho w_0 \delta_T^{**}/\mu_0$, while the thickness of the energy losses δ_T^{**} is determined according to (1.2). The Reynolds number is found from the solution of the integral energy equation and for q_w = const has the form

$$\mathrm{Re}_T^{**} = 0.0306\,\mathrm{Re}_z^{0,8}\,(\Psi_\varphi \Psi_C \Psi_T)^{0,8}\,\mathrm{Pr}^{-0,6}\left(\frac{\mu_w}{\mu_0}\right)^{0,2}. \tag{3.3}$$

The simultaneous solution of (3.1)-(3.3) and (1.10), (1.11) gives the working dependence for the coefficient of heat and mass transfer

$$\mathrm{St} = 0,0306\,\mathrm{Re}_z^{-0,2}\left\{\cos\varphi_m^{-0,75}\left[1 + 1,8\cdot 10^3 \frac{\delta_T^{**}}{R_0}\sin\varphi_m \frac{\delta_m}{\delta}\times\right.\right. \tag{3.4}$$
$$\left.\left.\times\left(1 + \frac{\psi - 1}{2(\psi n + 1)}\right)\right]^{0,162}\Psi_T\right\}^{0,8}\left(\frac{\mu_w}{\mu_0}\right)^{0,2}\mathrm{Pr}^{-0,6}.$$

The value of the twist angles of the flow at the wall, appearing in Eq. (3.4), is calculated from the relations (1.9) or (2.11).

Figure 4 shows the data on the heat transfer under conditions close to isothermal conditions in the twisted screen [2] for m = 0.5 and φ_S = 0; 58; 74° (points 1-3); the lines were calculated using the formula (3.4). It is evident that the calculation satisfactorily describes the increase in the heat transfer as the twist angle increases. In addition, this

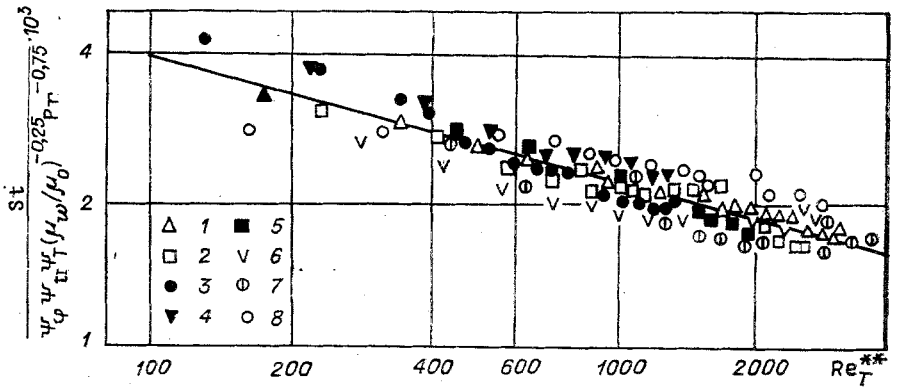

Fig. 5

excess for the initial sections of the channel equals 200-300%, while the twisting decays downstrean and its effect decreases.

Figure 5 shows a generalization of the experimental data for heat and mass transfer for isothermal, strongly nonisothermal, nontwisted, and completely twisted flows. The calculation of the heat and mass transfer in completely twisted flows also can be carried out based on Eq. (3.4), using in this case the experimentally determined local values of the twist angle of the flow at the wall, $Re_z = \rho_0 w_0 z/\mu$ and δ_T^{**}. The experimental data in Fig. 5 correspond to the following conditions: completely twisted flows [12]: 1) $\psi = 7$, $\psi = 32°$; 2) 7, 45°; 3) 7, 0°; partially twisted flows [1]: 4) $\psi = 7$, $\varphi_s = 58°$, $m = 0.8$; 5) 7, 74°, 0.68; quasiisothermal screens [2]: 6) $\psi = 1, 2$, $\varphi_s = 58°$, $m = 0.5$; 7) 1, 2, 58°, 0.9; 8) 1, 2, 0°, 0.5.

The experimental data in Fig. 5 are scaled to standard conditions with the help of the relation

$$St_0 = St/[\Psi_\varphi \Psi_c \Psi_T (\mu_w/\mu_0)^{0,25} Pr^{-0,75}].$$

It is evident this analysis generalizes the experimental results and they agree with the computed dependence for the standard boundary layer (3.2), indicating that the assumptions made in the analysis of complex phenomena studied here are correct.

Thus simple dependences were obtained for the calculation of the dynamic and thermal characteristics of nonisothermal twisted screens. An analogy was established between the effectiveness of the screen and the decay of its twist angle along the channel. The rotation of the screen appreciably affects the law of friction, the longitudinal velocity profile, and the coefficient β. The combined effect of these factors on the effectiveness of rotating gaseous screens is, however, weak. Twisting of the jet near the wall in this case intensifies the turbulent heat and mass transport toward the surface in the initial sections of the channel.

LITERATURE CITED

1. É. P. Volchkov, S. Yu. Sootar', and V. I. Terekhov, "Mass transfer on a burning surface under conditions of a twisted gas screen," in: Structure of the Boundary Layer at the Wall [in Russian], Novosibirsk (1978).
2. N. A. Dvornikov, V. P. Lebedev, and N. E. Shishkin, "Twisted gas curtain in a cylindrical channel," in: ibid.
3. N. E. Shishkin, "Distribution of the temperature and gas velocity in a pipe with jet mixing in a twisted flow," in: Vortex Effect and its Commercial Applications [in Russian], Kuibyshev Aviation Institute, Kuibyshev (1981).
4. E. P. Sukhovich, "Convective heat transfer under condition of turbulent mixing of bounded coaxial jets," Izv. SO Akad. Nauk SSSR, No. 3, Ser. Tekhn. Nauk, No. 1 (1978).
5. M. F. Zhukov, A. S. An'shakov, I. M. Zasypkin, et al., Electric-Arc Generators with Interelectrode Inserts [in Russian], Nauka, Novosibirsk (1981).
6. S. S. Kutateladze and A. I. Leont'ev, Heat and Mass Transfer and Friction in a Turbulent Layer [in Russian], Energiya, Moscow (1972).
7. É. P. Volchkov, N. A. Dvornikov, and V. I. Terekhov, "Heat and mass transfer and friction in a turbulent boundary layer of a twisted flow," Preprint No. 107-83, Institute of Thermal Physics, Academy of Sciences of the USSR, Siberian Branch, Novosibirsk (1983).

8. N. A. Dvornikov and V. I. Terekhov, "Transport ofmomentum and heat in a turbulent boundary layer on a curvilinear surface," Zh. Prikl. Mekh. Tekh. Fiz., No. 3 (1984).
9. A. J. Reynolds, Turbulent Flows in Engineering Applications [Russian translation], Energiya, Moscow (1979).
10. É. P. Volchkov, Gas Screens on Walls [in Russian], Nauka, Novosibirsk (1985).
11. É. P. Volchkov, V. P. Lebedev, and N. E. Shishkin, "Experimental study of a gas screen in a pipe," Izv. SO Akad. Nauk SSSR, Ser. Tekh. Nauk, No. 3 (1983).
12. É. P. Volchkov, S. Yu. Spotar', and V. I. Terekhov, "Turbulent mass transfer in the initial section of a pipe under conditions of twisting of the flow," in: 6th All-Union Conference on Heat and Mass Transfer, Minsk (1980), Vol. 1, Part 3.

DYNAMICS OF THE BEHAVIOR OF A GAS-BUBBLE NUCLEUS IN A HETEROPHASE MEDIUM

V. N. Popov and A. N. Cherepanov

UDC 669.18:532.529

The behavior of the nucleus of a gas bubble in a heterophase medium is an important problem in the investigation of the evolution of gas-shrinkage porosity in alloys crystallized in a certain temperature interval [1-4] and in a study of dynamical and mass-transfer phenomena in gas–liquid systems moving through a porous disperse media [5-8]. The general solution of this type of problem under the conditions of inhomogeneity of the temperature and concentration fields and in the presence of convection motions of the liquid phase poses a complicated mathematical problem. We therefore confine the ensuing discussion to a simplified mathematical model of the growth of the nucleus of a gas bubble in a homogeneous quasiequilibrium zone of a binary alloy [9], generalizing the solution to the case of the growth of a gas bubble in an isothermal liquid-saturated porous disperse medium.

We consider the crystallization of a binary alloy containing dissolved gas. We assume that the volume occupied by the alloys is small enough for the internal thermal resistance of the substance to be neglected in comparison with the external thermal resistance and for the crystallization of the alloy to be regarded as a volume process. We neglect shrinkage effects in crystallization, assuming that the nucleation of a bubble is associated with the displacement of dissolved gaseous component by the growing solid phase, while the motion of the melt is elicited by the variation of the gas-bubble radius due to gas diffusion from the intercrystalline liquid. We also assume that the vapor density in the bubble interior is negligible in comparison with the density of the gas, the distance between the centers of the bubbles is much larger than the characteristic diameter d_1 of the dendritic (structural) cell, and the diameter $2r_p$ of the bubble itself is so small that the convective diffusion of the gas toward the bubble surface as a result of its ascension can be disregarded. The equations of continuity and momentum transfer have the following form in a spherical coordinate system attached to the center of the bubble [9]:

$$\frac{\partial}{\partial r}(r^2 f_l u) = 0; \tag{1}$$

$$\rho\left(\frac{\partial u}{\partial t} + u\frac{\partial u}{\partial r}\right) = -\frac{\partial p}{\partial r} - \frac{\mu f_l u}{K_p(f_l)} + \frac{\mu}{r^2}\left[\frac{\partial}{\partial r}\left(r^2\frac{\partial u}{\partial r}\right) - 2u\right], \tag{2}$$

where u is the velocity of the liquid, f_ℓ is the cross section of the liquid phase (porosity), p is the pressure in the liquid, $K_p(f_\ell)$ is the permeability of the heterogeneous zone, ρ is the density of the liquid, μ is the dynamic viscosity of the liquid, and r is the radial coordinate. Equations (1) and (2) must be integrated subject to the boundary conditions on the surface of the bubble ($r = r_p$):

Novosibirsk. Translated from Zhurnal Prikladnoi Mekhaniki i Tekhnicheskoi Fiziki, No. 4, pp. 68-76, July-August, 1986. Original article submitted June 17, 1985.

 0021-8944/86/2704-0538$12.50